Bull Earthquake Eng (2015) 13:2547–2566
DOI 10.1007/s10518-015-9736-z

ORIGINAL RESEARCH PAPER

Dynamic response of a flexible rectangular underground structure in sand: centrifuge modeling

Deniz Ulgen · Selman Saglam · M. Yener Ozkan

Received: 2 February 2014 / Accepted: 17 February 2015 / Published online: 18 March 2015

Abstract Major earthquakes such as Kobe (1995), Kocaeli (1999) and Chi–Chi (Taiwan) have shown that underground structures have suffered significant damage due to dynamic loading. Therefore, recently, much priority has been given to seismic safety of underground structures located in earthquake-prone regions. There is, however, not much experimental research on the dynamic response of buried structures. This research aims to better understand the dynamic behavior of relatively flexible rectangular underground structures embedded in dry sand. To achieve this purpose, a series of dynamic centrifuge tests were conducted on a box-shaped flexible underground structure under harmonic motions with different accelerations and frequencies. Thus, response of soil and buried structure model was examined considering the dynamic soil structure interaction. Accelerometers were placed in the soil and on the buried structure model to evaluate the shear strain and acceleration response. Moreover, a special attempt was made to investigate the racking deformations by installing extensometers inside the tunnel model. Measurements obtained from those extensometers were compared with the predictions of analytical solutions. Results show that, Penzien's approach gives reasonable estimates of racking deformation for the rectangular shaped flexible underground structure.

Keywords Rectangular underground structure · Model test · Centrifuge test · Flexible tunnel · Racking deformation · Soil-structure interaction

D. Ulgen (✉)
Department of Civil Engineering, Mugla Sıtkı Kocman University, 48100 Mugla, Turkey
e-mail: denizulgen@gmail.com

S. Saglam
Adnan Menderes University, Aydın, Turkey

M. Y. Ozkan
Middle East Technical University, Ankara, Turkey

1 Introduction

Underground structures such as culverts, tunnels, subways or pipelines play a crucial role in achieving sustainable urban development. Recently, much attention has been given to the seismic safety of underground structures on the basis of experience gained from past earthquakes in Kobe, Japan (1995), Kocaeli, Turkey (1999) and Chi–Chi (Taiwan). Reports from these earthquakes (Sitar 1995; Iida et al. 1996; Power et al. 1998; Wang et al. 2001; Hashash et al. 2001) show that several buried structures suffered severe damage or collapsed due to seismic loading. This assessment confirms the need for further research on the seismic design of underground structures.

Seismic damage to underground facilities can be caused by fault actions, slope failures, liquefaction, as well as by deformations due to racking or ovaling tunnel section, axial compression and extension and longitudinal bending (e.g., Hashash et al. 2001). Racking deformation induced by transverse shear waves is the most common cause of damage to embedded structures with rectangular cross section (Penzien 2000). There exist two main analytical approaches used to estimate racking deformation of rectangular type embedded structures, namely the free field and the soil-structure interaction approaches. In the free field approach, the structure is assumed to have same stiffness as that of the surrounding ground. In other words, the structure conforms to soil deformations during shaking. This may lead to underestimation or overestimation of deformation depending on the relative stiffness between the underground structure and the soil (Wang 1993). Wang (1993), Penzien (2000), Huo et al. (2006), Bobet el al. (2008) proposed methodologies to overcome this problem by considering soil-structure interaction effect. In the soil-structure interaction approach, racking deformations are estimated based on relative stiffness and free-field deformations. Sectional forces induced by racking deformations are then calculated by means of static analysis. Dynamic soil structure interaction is not dealt with in this approach. In order to capture the dynamic effects, numerical methods have been applied for the analysis of underground structures.

Seismic performance of embedded structures has been frequently studied by means of the small scale models using 1 g shaking tables. However, gravitational body force can not be properly represented in such models. Physical modeling within geotechnical field is governed by complex stress dependent behavior, especially in soil-structure interaction. Thus, the gravitational force must be well represented during the model tests. Although this problem can be overcome in full scale tests, construction of prototype is impractical and economically unfeasible. The centrifuge technique, hence, becomes an alternative solution in which the small scale models are tested within an increased gravity field for simulating the actual stress conditions in prototype scale. Some centrifuge studies regarding faulting effects on buried pipelines and dynamic behavior of underground structures in liquefied soils have been reported in the literature (O'rourke et al. 2003; Ha et al. 2010; Ling et al. 2003; Chian and Madabhushi 2012). Moreover, ovaling deformation mode of buried structures under vertically propagated shear waves were investigated by Cilingir and Madabushi (2011a, b) and Lanzano et al. (2012). The researches mostly focused on the acceleration response of soil, dynamic earth pressures and the effect of depth on seismic response of circular tunnels. There are only a few research studies (e.g., Cilingir and Madabushi 2011c; Pitilakis et al. 2013; Dashti et al. 2013) on racking deformation modes and dynamic behavior of rectangular underground structures. Cilingir and Madabushi (2011c) performed dynamic centrifuge tests and finite element analyses to understand the effect of depth on the seismic response of square tunnels. The authors reported that ratio between accelerations over the tunnel and at the base increases when the tunnel is

embedded at shallow depths. However, the deformations in shallow and deep tunnel models were reported not to show significant difference. Pitilakis et al. (2013) carried out centrifuge tests to investigate the dynamic behavior of shallow square tunnels with different rigidities in soft soils. The results of the experimental tests on the flexible tunnel showed that the tunnel vibrates in rocking mode and the dynamic pressures are higher near the corners than at the middle of sidewall. In the studies of Pitilakis et al. (2013) and Cilingir and Madabushi (2011c), the displacements of tunnel were measured indirectly by using the accelerometers. This may cause unanticipated errors or misleading results due to the probable rocking response of the tunnel. Besides, there is no experimental study available elucidating the deformation mechanism of the tunnels with directly measured sidewall displacements. In other words, lack of experimental data is one of the main reasons to insufficient clarification of load transfer and deformation mechanisms of rectangular buried structures. Generally, stiff structures on soft soils have been investigated. The dynamic response of embedded structures with flexible sides, which are to be subjected to shear stresses (Clough and Penzien 1993), is scarcely mentioned. More experimental research is needed to develop and validate design methodologies for flexible underground structures subjected to seismic loading.

In the present study, a series of centrifuge tests were performed to assess the dynamic behavior of box-shaped flexible culvert buried in dry sand. Plane strain conditions were reproduced in the tests thus limiting the study to racking deformation modes induced by seismic waves. The response of soil and deformation mechanism of the buried structure are investigated and discussed. Measured racking deformations are compared with those estimated using the approaches proposed by Penzien (2000) and Bobet et al. (2008). Although there exist shortcomings of these analytical solutions, they provide significant insight about racking deformations of rectangular underground structures. In both approaches, the soil and the tunnel are assumed to behave elastically whereas it may not be valid for practical problems. The equations of these procedures are derived by neglecting the slip at the soil-structure interface. Both approaches employ the pseudo-static method by assuming an isotropic and homogeneous ground. There is a significant difference between the approaches in terms of load transfer mechanism. The solution proposed by Penzien (2000) involves only the effect of shear stress acting on the perimeter of the structure whereas the solution suggested by Bobet et al. (2008) involves the effects of both shear stress and normal stress.

2 Centrifuge test system

Model tests were conducted in IFSTTAR (Institut français des sciences et technologies des transports, de l'aménagement et des réseaux) using geotechnical beam centrifuge with an arm of 5.5 m in radius. The beam can rotate with a maximum of 200*g* centrifugal acceleration and has a payload capacity of 2000 kg-f. The swinging bucket attached at the end of the beam contains data acquisition, shaker and the model container. Harmonic or real earthquake motions can be applied in horizontal direction by means of one dimensional servo hydraulic shaker. The shaker supplies the excitations at the base of soil container. In order to minimize the boundary effects, an equivalent shear beam (ESB) container was used throughout the dynamic centrifuge tests. Madabhushi (1994), Zeng and Schofield (1996), Teymur and Madabhushi (2003) and Lee et al. (2013) studied the performance and the dynamic response of the ESB container in centrifuge tests. They verified that the ESB model container can be efficiently used to simulate the horizontal shear

deformations and the semi-infinite soil medium. The container has internal dimensions of 800 mm in length, 350 mm in width and 410 mm in depth. It consists of 14 horizontal layers of aluminium alloy separated by 4 mm thick rubber sheets. Side walls of ESB box are allowed to be free in shaking direction and restrained in transverse direction. Rough shear rods were used to resist the complementary shear stresses developed on the vertical face of the container. Results obtained from dynamic tests show that ESB box has resonant frequencies between 32 and 37 Hz (Escoffier 2008).

Data were recorded through high rate data acquisition system. As the system is placed into the bucket, the data are transmitted to control room through a ethernet-fiber optic system to the control room. Since the dimensions of the equipment placed into the model may significantly affect the results of the centrifuge tests, rather compact and lightweight piezoelectric type accelerometers were used during the tests. There were 26 accelerometers (Bruel & Kjear 4317) having natural internal bandpass filter of 1–20 kHz placed in the soil and on the outside face of tunnels. Total soil settlement was determined through measurements of the surface level using laser displacement sensors before and after shaking took place.

In order to measure the deformations of the box-type culvert, horizontal and diagonal extensometers developed by IFSTTAR were used in the tests. Horizontal extensometers designed on a fork shaped system are illustrated in Fig. 1a. Five pairs of horizontal extensometers piled reciprocally were used to measure horizontal shear deformations along the height of both sidewalls of the culvert model. Diagonal deformations were measured by means of the diagonal extensometer illustrated in Fig. 1b. In order to investigate the boundary effects due to the end walls and to examine the validity of plain strain conditions, extensometers were placed in the middle and near both ends of tunnel model.

A series of centrifuge tests were conducted to investigate the performance of ESB box at different centrifugal acceleration levels. Results showed that 40*g* was the most reasonable centrifugal acceleration to eliminate the boundary effects of the soil model. Accordingly, dynamic centrifuge tests were performed at a centrifugal acceleration of 40*g*. The scaling laws (Schofield 1980; Taylor 1995) between prototype and model were derived for a 40*g* centrifugal field.

Possible effects due to unscaled size of the soil particles are often neglected in centrifuge testing. Iglesia et al. (2011) suggested that the grain size effects can be minimized when the model dimensions are at least 20 times larger than the mean grain size, d_{50}. Ratio of model dimension to d_{50} for the present study is approximately 250, thus such effects can be ignored.

3 Physical characteristics of soil and preparation of model ground

Centrifuge model tests were performed by using dry Fontainebleau sand having round shaped particles of uniform fine quartz with a mean diameter of 0.2 mm. The maximum and minimum dry unit weights of soil are 16.78 and 13.93, corresponding to minimum and maximum void ratio values of 0.55 and 0.86, respectively. Li et al. (2013) carried out centrifuge tests to identify the dynamic properties of Fontainebleau sand. In the study, centrifuge test data were fitted to general empirical equations developed by Ishibashi and Zhang (1993). The present study borrowed the shear modulus degradation curves constructed for the Fontainebleau sand from the research results of Li et al. (2013). Empirical formulae proposed for the determination of shear modulus degradation (G/G_{max}) and damping ratio (D) (Eqs. 1, 2, 3) were given as:

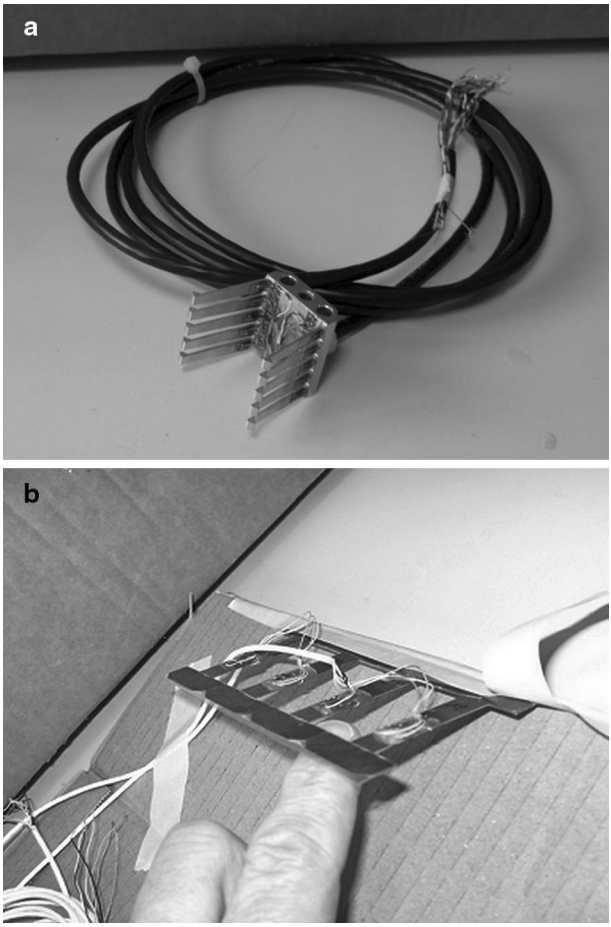

Fig. 1 A view of **a** horizontal extensometer and **b** diagonal extensometer

$$\frac{G}{G_{\max}} = K(\gamma)\sigma_c^{m(\gamma)-m_0} \tag{1}$$

$$K(\gamma) = 0.5\left[1 + \tanh\left\{\ln\left(\frac{0.000102}{\gamma}\right)^{0.613}\right\}\right] \tag{2}$$

$$m(\gamma) - m_0 = 0.34\left[1 - \tanh\left\{\ln\left(\frac{0.000556}{\gamma}\right)^{0.4}\right\}\right] \tag{3}$$

where γ is the shear strain.

The maximum shear modulus of the Fontainebleau sand can be estimated by using the following empirical relationship (Eq. 4) proposed by Hardin and Drnevich (1972) (Li et al. (2013):

$$G_{\max} = 3230 \cdot \frac{(2.973 - e)^2}{(1 + e)} \cdot OCR^k \cdot \left(\sigma'_m\right)^{1/2} \tag{4}$$

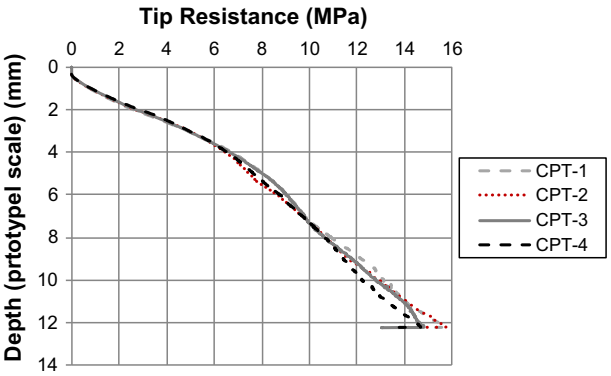

Fig. 2 Variation of cone penetration resistance with depth

where G_{max} is the maximum shear modulus in kPa, e is the void ratio, OCR is the ratio of maximum past effective stress to current effective stress, k is an overconsolidation ratio exponent and σ'_m is the effective confining pressure in kPa. For a void ratio of 0.64 and an effective confining pressure of 28 kPa the maximum shear modulus at the mid-depth of the culvert model was approximately calculated as 56,500 kPa.

Air pluviation technique was utilized to construct the model ground throughout the centrifuge testing. In order to have uniform soil density, dry sand was filled into the container by dropping it from a fixed height of 60 cm. Density control boxes were placed into the soil and in-flight cone penetration tests (CPT) suggested by Bolton et al. (1999) were performed to check the homogeneity and repeatability of the prepared soil model. Details of the procedure and working principles of CPT are given by Bolton et al. (1999) and Ali et al. (2010). Figure 2 shows the variation of cone penetration tip resistance with depth. Measurements obtained from the density control boxes and CPT indicate that uniform and reproducible model grounds with a relative density of 70 % were achieved in the centrifuge tests.

4 Culvert model

An aluminum box-shaped underground structure model was manufactured for the dynamic centrifuge tests. Electro-erosion technology was utilized in the manufacturing process. Thus, it was possible to eliminate residual stresses and strains. The model is 47 mm (in prototype scale 1.88 m,) by 50 mm (in prototype scale 2.0 m) in cross section and 350 mm (in prototype scale 14 m) in length. Thicknesses of sidewalls and slabs are 1.5 mm (in prototype scale 0.06 m) and 6 mm (in prototype scale 0.24 m), respectively. In order to minimize bending effects, roof and invert slabs are kept relatively thick as compared to that of sidewalls. The top and bottom slabs of the model were located at a depth of 50 mm (in prototype scale 2 m) and 200 mm (in prototype scale 4 m). Figure 3 shows the cross section view of the under-ground structure model.

Extremities of the culvert model and ESB box were designed to satisfy plane strain conditions and to achieve free movement without any stress. The neoprene foams were placed at the ends of model, and longitudinal sides of the ESB box was covered with Teflon sheet. Hence, free movement of box-shaped underground structure model was

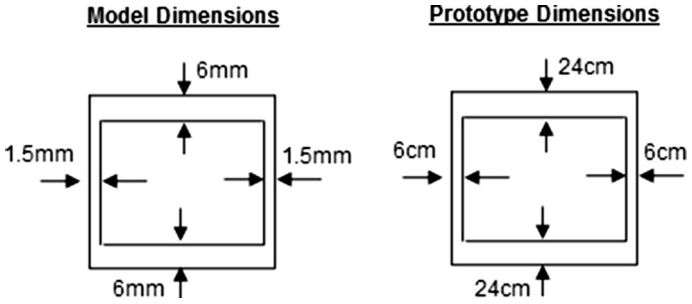

Fig. 3 Cross section of culvert model

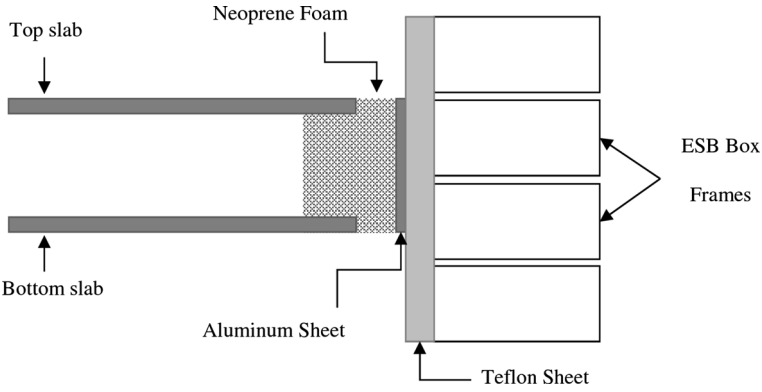

Fig. 4 Schematic drawing of the designed extreme section

enabled by minimizing the friction between tunnel and container. Schematic drawing of the designed extreme section is given in Fig. 4 (Ozkan et al. 2013).

5 Test instrumentation

In order to investigate various aspects of dynamic response of buried culverts, instrumentation set up was designed to gather as much data as possible. As seen in Figs. 5 and 6, a set of accelerometers were buried to examine acceleration response in soil and free field response. Boundary conditions and effects of the box on the tests were examined using six accelerometers mounted on ESB box and one accelerometer located over the shaking table. The accelerometers were placed in vertical arrays labelled V1, V2, V3, V4 at various distances. In addition, three laser displacement sensors were positioned over the container to measure the soil settlement at the surface (Fig. 7a).

There were five accelerometers placed on the external surface of the culvert model as well. Horizontal accelerations in shaking direction were recorded by two of them located in the central section, one at the bottom and one at the top level of the sidewall. Three more horizontal accelerometers were mounted at each end of the culvert model (Fig. 7b). These accelerometers were used to check whether plain strain behaviour was maintained or not.

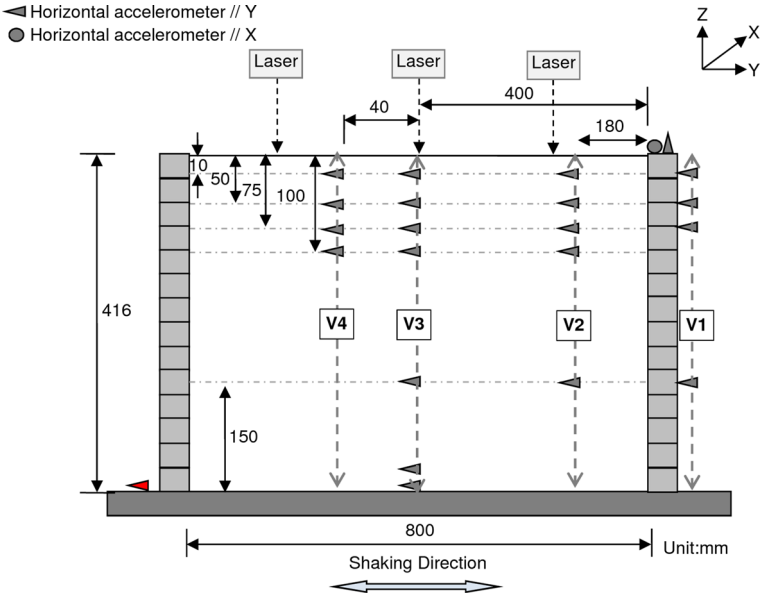

Fig. 5 Schematic illustration of test instrumentation in free-field tests (without structure)

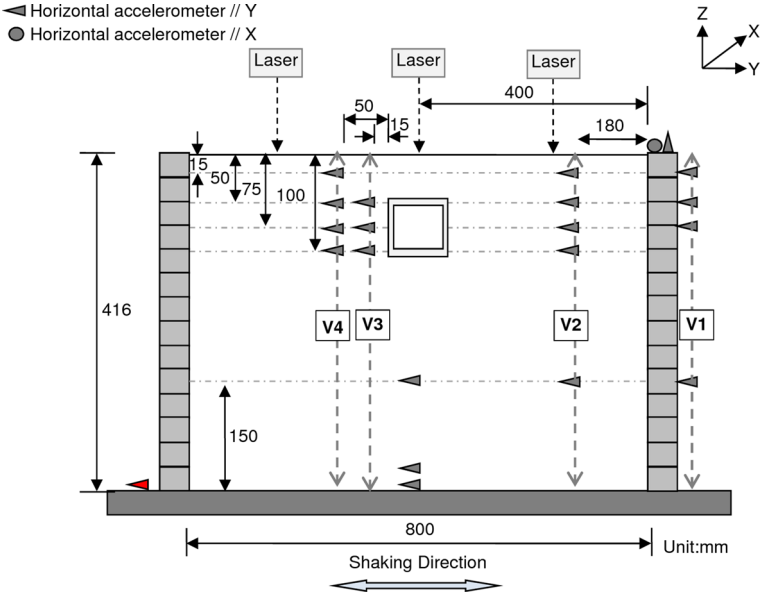

Fig. 6 Schematic illustration of test instrumentation in model tests (with structure)

The response of the sidewalls was monitored through the extensometers placed inside the culvert. Position of these extensometers is illustrated in Fig. 8. The transverse deformation of the sidewalls was measured by means of five pairs of horizontal extensometers mounted at the central section. Furthermore, the deformations of the culvert diagonal were

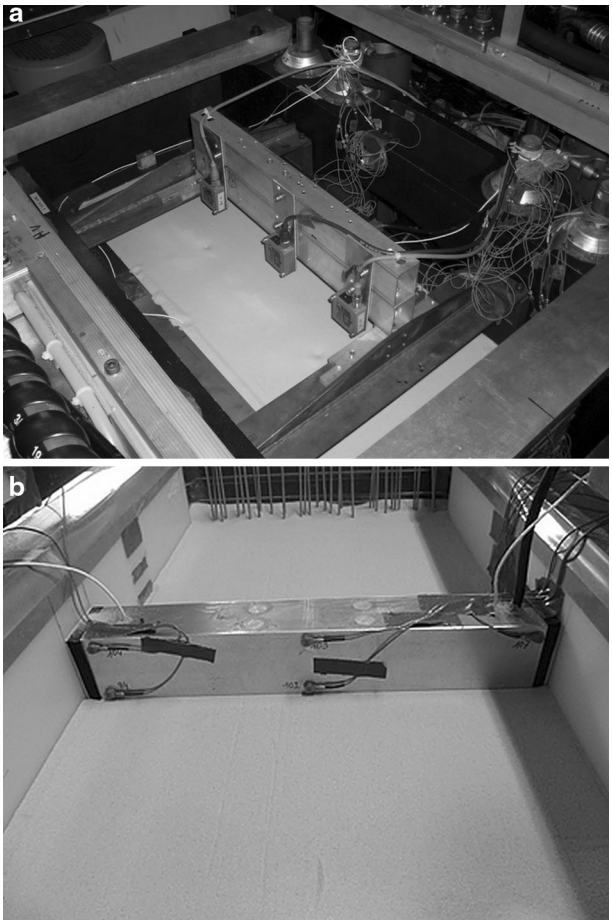

Fig. 7 Instrumentation **a** Laser displacement sensors **b** accelerometers placed on the culvert model

measured by using the diagonal extensometers. Two of the diagonal extensometers were located near the centre while the other two were located near the ends of the culvert. Those located near the ends can also be used to check whether plain strain behaviour is valid under dynamic loading. A schematic illustration of the deformed shape of the culvert model is given in Fig. 9. Although the given deformed cross sections represent perfectly hinged corners without any elongation of sidewalls or slabs, the aluminium sidewalls may be subjected to bending. Since the change in diagonal length may not totally reflect the sidewall deformations induced by bending, the deformations measured by horizontal extensometers (Δ_{HE}) can provide a clearer insight in dynamic response of the sidewalls.

6 Testing program

Two free field and four dynamic centrifuge tests with culvert model were conducted under a centrifugal acceleration of 40*g*. The free field motions were carried out using prototype accelerations of 0.25 and 0.4 g, and frequencies of 2 and 3.5 Hz, respectively. The culvert

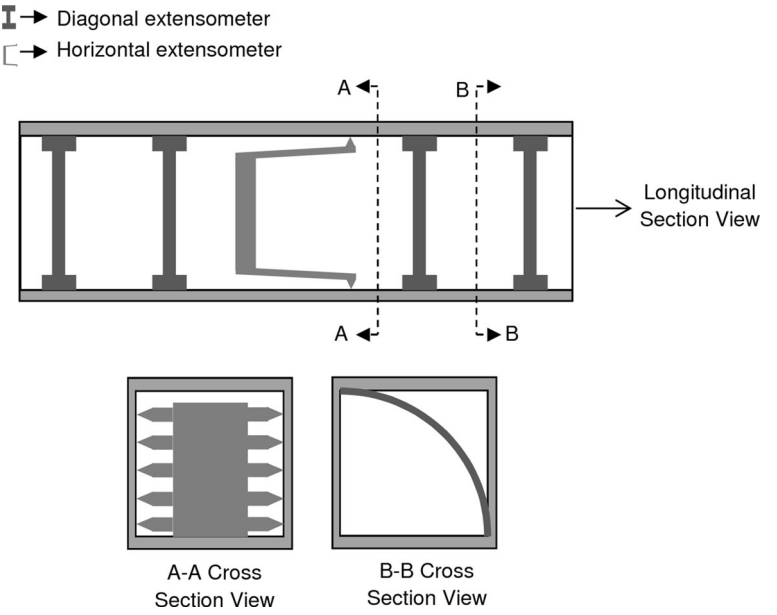

Fig. 8 Layout of extensometers placed inside the culvert model

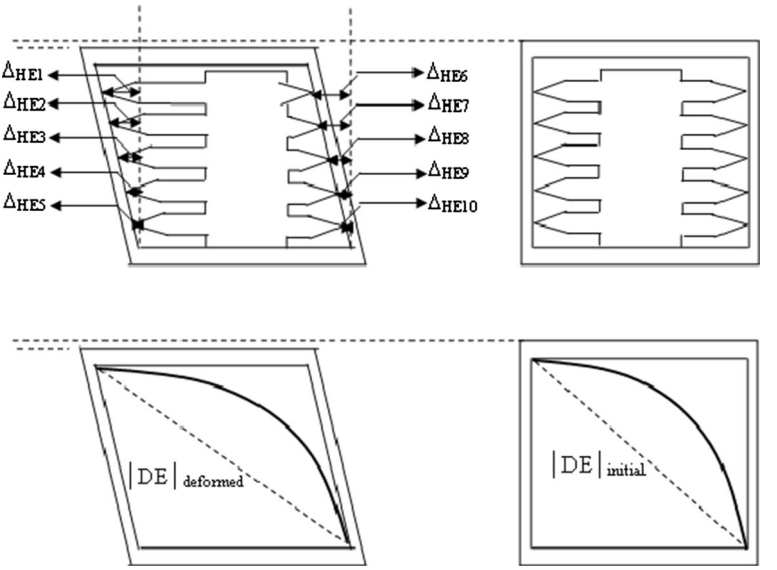

Fig. 9 Deformed cross sections of culvert model

model was tested under four different harmonic motions. The target input accelerations and the ones measured at the shaking table are indicated in Table 1. The measured accelerations are slightly higher than the specified target, with differences in the range of 0–18 %.

Table 1 Dynamic centrifuge testing program

Test number	Explanation	Target input acceleration (prototype) (g)	Measured input acceleration (prototype) (g)	Frequency (prototype) (Hz)	Duration (prototype) (s)
1	No culvert: free-field	0.25	0.25	2	35.2
2	No culvert: free-field	0.4	0.46	3.5	20
3	With culvert	0.25	0.28	2	35.2
4	With culvert	0.25	0.27	3.5	20
5	With culvert	0.4	0.47	2	35.2
6	With culvert	0.4	0.42	3.5	20

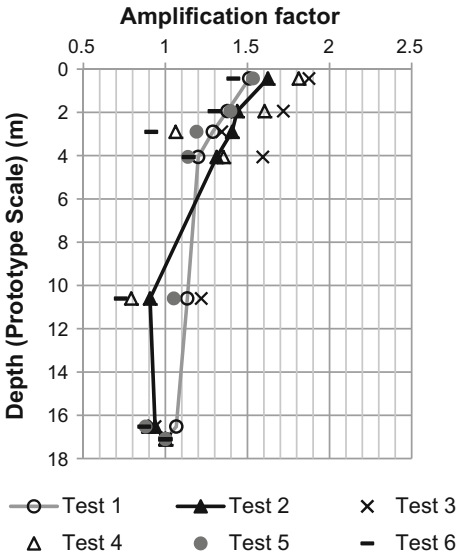

Fig. 10 Variation of amplification factors for the tests with and without culvert model

7 Test results and discussion

7.1 Amplification

Amplification factor is defined herein as the ratio of maximum acceleration recorded in the soil to the maximum input acceleration recorded at the base of soil model. Maximum acceleration amplifications through the soil profile (Fig. 10) were determined using the accelerometer arrays V3 (Fig. 5) and V2 (Fig. 6) in the absence (given by continuous lines with markers) and presence (given by markers) of underground structure model, respectively. As seen in Fig. 10, the maximum horizontal acceleration increases gradually from base of ESB box to 4 m below surface, but then a remarkable increase in amplification takes place just below the surface. The maximum amplification occurs near the surface and varies between 1.4 and 1.8.

There are slight differences between maximum accelerations measured at the base of the model ground (a_{base}) and those of input motions (a_{input}) in all the tests. The ratios

($a_{base}/a_{input,}$) vary approximately in the range from 0.9 to 1.2. This indicates that there may be a negligible amount of sliding along the interface between the soil and container.

7.2 Surface settlements

The surface settlements after shaking were measured by means of laser displacement sensors at three different locations as shown in Fig. 7a. The settlements observed according to the sensor positions are given in Table 2. Similar values of settlements observed at different locations point out a homogeneous settlement along the soil profile. Hence, the surface settlement at the end of the test can be reported as average values. Average settlement increases from 4.3 to 4.5 mm (17.2–18.0 cm in prototype scale) to 5.9–7.5 mm (23.6–30.0 cm in prototype scale) in model scale with increasing input acceleration and cyclic shear strain levels. Studies performed by Silver and Seed (1971) and Tokimatsu and Seed (1987) showed that the settlement of dry sands under cyclic loading is mainly depend on the cyclic shear strain, number of cycles and relative density of soil. Pitilakis et al. (2013) performed centrifuge tests on tunnels buried in dry sand with a relative density of 50 %. The obtained average vertical strains were varied approximately from 1.5 to 2 %. In the present study, although the initial relative density and the loading conditions were not similar to those of the study by Pitilakis et al., average vertical strains were in the range of 1–1.8 %. Corresponding increase in the relative density was between 5 and 10 %. Besides, the average vertical strains were estimated between 1 and 2 % using the curves recommended by Silver and Seed (1971). Thus, it can be noted that the predictions of Silver and Seed (1971) are in agreement with the results obtained from this study.

7.3 Shear strains

Shear strains can be obtained from displacement time histories calculated through double integration of the recorded acceleration data. The procedure proposed by Zeghal and Elgamal (1994) was used for the evaluation of shear strains. If there is a vertical array consisting of three or more accelerometers, second order approximation (Zeghal and Elgamal 1994) can be used to evaluate shear strain at depth z_i as follows:

$$\gamma(z_i) = \frac{\left[(d_{i+1} - d_i)\frac{(z_i - z_{i-1})}{(z_{i+1} - z_i)} + (d_i - d_{i-1})\frac{(z_{i+1} - z_i)}{(z_i - z_{i-1})}\right]}{(z_{i+1} - z_{i-1})} \tag{5}$$

where, γ is the shear strain and d_i is the integrated displacement. Free-field shear strains plotted in Fig. 11 were calculated using the accelerometer arrays (V1, V2, V3, V4) shown in Fig. 5. Results of Test 1 and Test 2 show that shear strain levels around culvert model vary between approximately 0.2 and 0.6 %. Figure 12 shows the computed shear strains in the presence of culvert model using the accelerometer arrays (V1, V2, V3, V4) shown in Fig. 6. In Test 5, acceleration data of V1 could not be measured due to sensor malfunctioning. Strain levels seem to be in good agreement with those obtained from free-field tests which were conducted under similar input motion of the tests with the model (i.e. Test 3 and Test 6). Maximum shear strain is approximately 1 % when the input motion has a prototype acceleration of 0.47 g and a frequency of 2 Hz. Li et al. (2013) stated that the resonant frequency of the model ground was close to 3.5 Hz at low strain levels (mostly lower than 0.005 %). However, it is observed that strain level has a tendency to increase when the model is vibrated with a frequency of 2 Hz. This may be due to a decrease in the natural frequency of the model due to the shear modulus degradation during shaking.

Table 2 Surface settlements (model scale) recorded by laser displacement sensors

Tests #	Surface settlement (mm) (left side)	Surface settlement (mm) (center)	Surface settlement (mm) (right side)	Average settlement (mm)
3	4.2	4.1	4.7	4.3
4	4.3	4.6	4.5	4.5
5	7.4	8.0	7.0	7.5
6	6.0	5.7	6.0	5.9

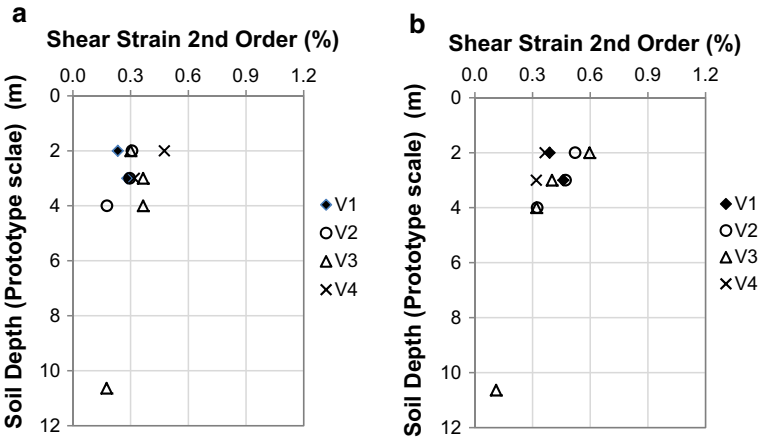

Fig. 11 2nd order shear strains in the absence of culvert model **a** Test 1 **b** Test 2

Therefore, nonlinear behavior of soil at large strains can shift the resonant frequency closer to 2 Hz.

7.4 Sidewall deformations

The deformations along the culvert models were measured using the horizontal and diagonal extensometers. The diagonal extensometers were placed in longitudinal direction of the tunnel as shown in Fig. 8, and they were used to examine the validity of plain strain conditions. It was observed that the diagonal deformations measured at different locations in longitudinal direction were quite consistent. Thus, the validity of plain strain conditions was verified.

There were 10 extensometers arranged in pairs mounted inside of the underground structure model. These extensometers were used to measure horizontal shear deformations at different heights on the sidewalls. They were labeled from HE1 to HE10 (Fig. 9). Although cyclic deformations at the left and right sidewalls are not exactly equal to each other, records were reasonably consistent. Such slight differences might occur due to the super sensitivity of extensometers used in centrifuge testing. Horizontal deformation at top slab level (HE1, HE6) was observed to be the highest while it was almost zero at the bottom (HE5, HE10). Nevertheless, the increase in horizontal deformation from bottom to top mostly starts to decrease after mid-height of the sidewalls. In order to provide a clear illustration of horizontal deformations recorded by different extensometers, horizontal deformations recorded between 15th and 16th seconds of the loading are shown in Fig. 13.

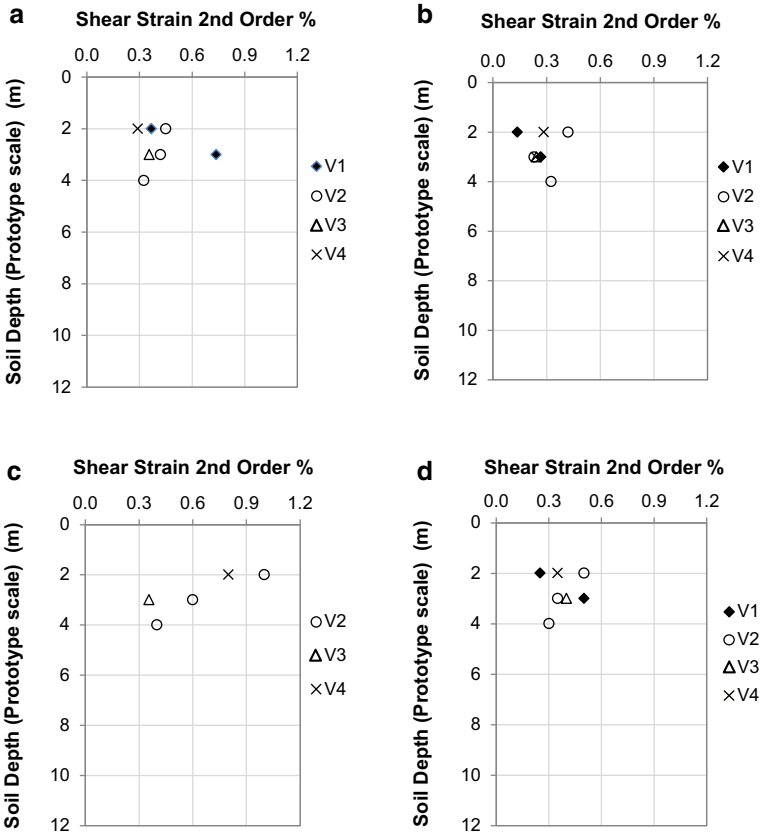

Fig. 12 2nd order shear strains in the presence of culvert model **a** Test 3 **b** Test 4 **c** Test 5 **d** Test 6

The reciprocal extensometers record opposite signals of almost the same absolute values of deformations. Some of data were missing due to noise in the data acquisition system or measurement errors. During cycling, the surrounding soil sustains active state at one side and passive state at the other side. Differences between the horizontal shear deformations recorded by the reciprocal extensometers can, therefore, be attributed to the interaction between the sidewalls and the soil.

7.5 Racking deformations

The deformations of the model were directly measured using horizontal extensometers. Besides, racking distortions of the model were indirectly obtained from displacement time histories calculated by double integration of acceleration records. Having computed the free-field deformation at mid-depth of the model structure, the racking ratio (R) was calculated by the following formula:

$$R = \frac{\Delta_{str}}{\Delta_{ff}} \tag{6}$$

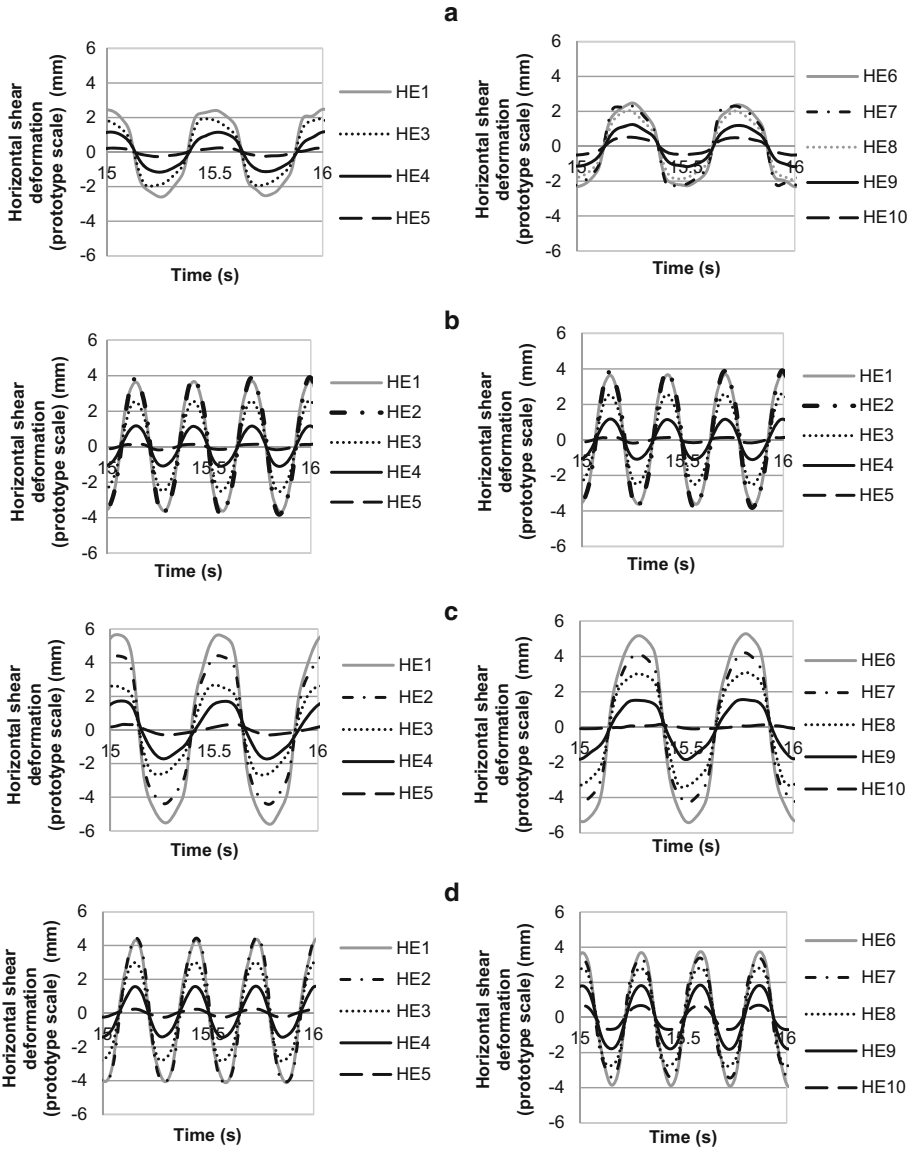

Fig. 13 Sidewall horizontal shear deformations recorded between 15th and 16th seconds of loading **a** Test 3 **b** Test 4 **c** Test 5 **d** Test 6

where, Δ_{str} is the racking deformation of underground structure, Δ_{ff} is the free-field deformation of underground structure. Comparison of racking ratios obtained from extensometers with those calculated using acceleration records is presented in Table 3. Racking ratios calculated from the records of accelerometers are relatively higher than those obtained by extensometers. It is believed that such high differences are caused by the existence of rocking motion or spurious accelerations generated by the vibration of system in X and Z directions.

Table 3 Comparison of racking ratios obtained from extensometers and accelerometers

Culvert model #	Test #	Racking ratio by extensometers	Racking ratio by accelerometers
1	3	0.64	1.89
1	4	1.16	1.40
1	5	0.50	1.87
1	6	0.72	1.07

Centrifuge test results were compared with the predictions of analytical solutions proposed by Penzien (2000) and Bobet et al. (2008) in terms of racking deformations. The estimated racking deformations are strongly dependent on the relative stiffness between the soil and underground structure (flexibility ratio) in both of these approaches. The flexibility ratio, F_R, is the ratio of shear modulus of surrounding ground to structural racking stiffness. Wang (1993) quantified the relative racking stiffness by the F_R and formulated as follows:

$$F_R = \frac{G_m \times W}{S \times H} \tag{7}$$

where, S is the force required for unit racking deformation, G_m is the degraded shear modulus, W and H is the width and height of the underground structure, respectively. Since the shear modulus decreases with increasing strain, different F_R values can be obtained under different dynamic motions for the same underground structure. Initial value of F_R is 11.3 and varies between 11.3 and 0.5 depending on the shear strain during shaking. F_R values were calculated according to the maximum shear strains during shaking, and corresponding values of shear modulus were estimated using shear modulus reduction curves provided by Li et al. (2013). Comparison of maximum sidewall deformations of the rectangular tunnel for different F_R values is presented in Fig. 14. The G_m values obtained from modulus degradation equations (Eqs. 1, 2, 3) were directly used in the procedure of Penzien (2000) whereas they were used as initial estimates of shear modulus in the procedure of Bobet et al. (2008). Since Bobet et al. (2008) suggests an iterative procedure to refine the shear modulus and corresponding shear strain, the values introduced in Fig. 14 are those come up at the end of iteration. A reduction in the initial estimates of shear modulus for the Tests 3, 4 and 6 and an increase in the shear modulus for Test 5 resulted by the iteration process. Correspondingly, the F_R values obtained in Penzien's (2000) and Bobet's et al. (2008) approaches do not perfectly match with each other. In a general sense, since the Bobet et al. (2008) developed the approach for the underground structures stiffer than the surrounding soil, conservative racking deformations were estimated for the flexible tunnel tested in this study. Bobet et al. (2008) approach tends to overestimate the racking deformations by a factor varying between 1.2 and 1.9. Considering that the stiffness of the structure is less than that of the surrounding soil, the closed-form solution proposed by Penzien (2000) gives more reasonable estimates when compared to the solution suggested by Bobet et al. (2008). The difference between the estimated deformations and the observed ones increases when the model is shaken by an input motion with a frequency of 2 Hz. As the measured sidewall deformations significantly increase under a frequency of 2 Hz, the soil-structure system may undergo resonance state. Although the analytical solutions do not take the effect of frequency into account, stiffness degradation curves in which the shear strains observed during the tests were taken into consideration in the course of analytical calculations. Considering the difference between the measured and the estimated deformations under a loading frequency of 2 Hz, such resonance shear

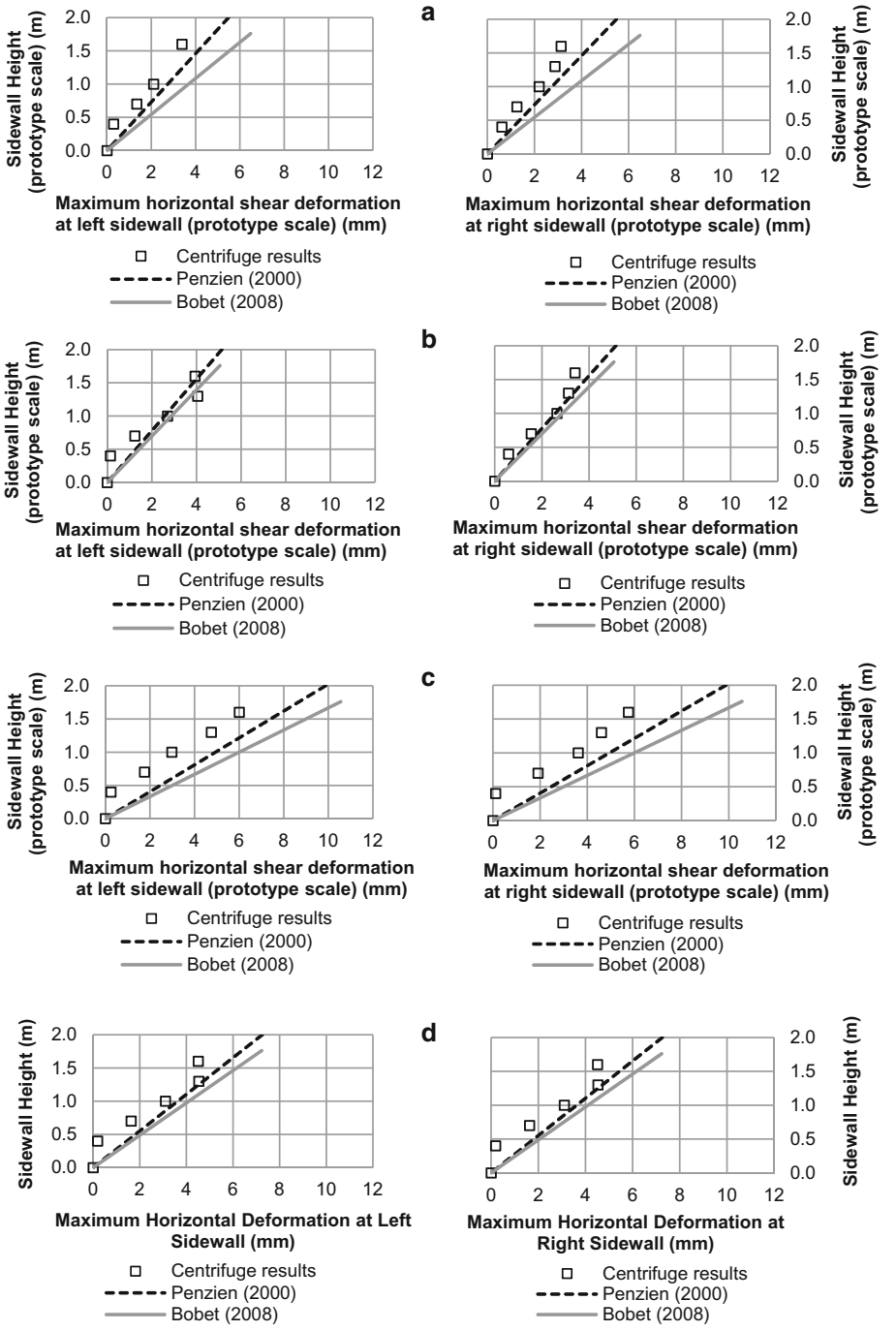

Fig. 14 Maximum horizontal shear deformations (prototype scale) recorded on sidewalls during **a** Test 3, $F_R = 1.1$ **b** Test 4, $F_R = 1.5$ **c** Test 5, $F_R = 0.5$ **d** Test 6, $F_R = 0.9$

strains may make the analytical approaches conservatively reflect the dynamic response in accordance with the nonlinear relationship between stiffness degradation and shear strain. In other words, the higher shear strains occur the more conservative analytical estimates may be observed for the flexible tunnels. Correspondingly, it can be said that the frequency range affecting the straining response of the system would change estimation performance of the analytical approaches. Therefore, the difference in racking deformations may be attributed to the effect of excitation frequency and the resonance frequency of the soil-structure system as stated by Pelli et al. (2006). Moreover, Cilingir and Madabushi (2011a, b, c) have emphasized the frequency effect on the dynamic response of the tunnels. They concluded that significant increases in amplification with varying fundamental frequency range for different centrifuge models used in the studies.

Another remarkable point seen in the plots given in Fig. 14 is non-linearity of the deformation path obtained during the tests. One of the shortcomings of the analytical approaches is the assumption of no slip on the interface between the soil and the structure. However, it may not be the case in practical problems due to varying stress concentration along the sidewall. These different stress concentrations along the sidewall are inherently induced by the flexibility of the tunnel that is lower than the surrounding soil at the beginning. The authors believe that such stress concentrations may correspondingly cause the sidewalls to undergo deformations on a non-linear path along the sidewall.

8 Summary and conclusions

There is a lack of experimental research to validate the current seismic design approaches proposed for rectangular underground structures. Hence, a series of dynamic centrifuge tests were conducted on a flexible box-type buried structure in dry sand under 40*g* centrifugal acceleration field. Centrifuge tests reproduced plain strain conditions to study the racking deformation modes induced by seismic waves in the culvert model; they were carried out using harmonic input motions with different accelerations and frequencies. Experimental data were analyzed in order to assess the dynamic response of rectangular underground structures with particular emphasis on racking deformations. Furthermore, the acceleration responses of soil and buried structure are discussed. The following conclusions can be drawn on the basis of the results obtained from the dynamic centrifuge tests.

1. The lateral sidewall deflection profiles observed in this study show reasonable agreement with theoretically predicted racking deformation schemes. There is an opposite phase between the recorded deformations by reciprocal extensometers. Although those deformations are not perfectly equal to each other, they are reasonably consistent.
2. The racking ratios computed using the acceleration records at the top and bottom slab of buried rectangular structure model are relatively higher than those obtained from the extensometers. The most likely reasons for those higher racking ratios might be existence of spurious accelerations caused by centrifuge shaker and/or rocking motion of the structure model.
3. The measured racking deformations in the dynamic centrifuge tests were compared with the analytical estimates proposed by Penzien (2000) and Bobet et al. (2008). Rather than those estimated by Bobet et al. (2008), the sidewall deformations estimated by Penzien (2000) method provide a remarkably good fit with the data obtained from centrifuge tests conducted on a flexible underground structure model which is less stiff than the surrounding soil.

4. The difference between the estimated deformations and the observed ones increases when the model is shaken by an input motion with frequency of 2 Hz. Since the closed form solutions do not consider the effect of frequency on the dynamic response of underground structure, a fundamental frequency of the model ground close to 2 Hz can be attributed as a possible reason for this observation.
5. The tests results reveal a non-linearly deformed shape of sidewalls whereas the estimations show linearly deformed sidewalls. Any possible slippage and according differential stress concentrations induced by F_R apart from 1 may cause the sidewalls to undergo deformations on a non-linear path.

Acknowledgments The research leading to these results has received funding from the European Union Seventh Framework Programme [FP7/2007–2013] under Grant Agreement No. 227887 [SERIES]. The authors would like to thank IFSTTAR centrifuge team for their valuable supports throughout the study.

References

Ali H, Reiffsteck P, Thorel L, Gaudin C (2010) Influence factors study of cone loading test in centrifuge. In: Proceedings CPT10, Huntington Beach, May

Bobet A, Fernández G, Huo H et al (2008) A practical iterative procedure to estimate seismic induced deformations of shallow rectangular structures. Can Geotech J 45(7):923–938

Bolton MD, Gui MW, Garnier J, Corte JF, Bagge G, Laue J, Renzi R (1999) Centrifuge cone penetration tests in sand. Geotechnique 49(4):543–552

Chian SC, Madabhushi SPG (2012) Effect of buried depth and diameter on uplift of underground structures in liquefied soils. J Soil Dyn Earthq Eng 41:181–190

Cilingir U, Madabhushi SPG (2011a) Effect of depth on the seismic response of circular tunnels. Can Geotech J 48(1):117–127

Cilingir U, Madabhushi SPG (2011b) A model study on the effects of ınput motion on the seismic behavior of tunnels. J Soil Dyn Earthq Eng 31:452–462

Cilingir U, Madabhushi SPG (2011c) Effect of depth on the seismic response of square tunnels. Soils Found 51(3):449–457

Clough RW, Penzien J (1993) Dynamics of structures, 2nd edn. McGraw Hill, New York

Dashti S, Hushmand A, Ghayoomi M, McCartney JS, Zhang M, Hushmand B, Mokarram N, Bastani A, Davis C, Yangsoo L, Hu J (2013) Centrifuge modeling of seismic soil-structure-ınteraction and lateral earth pressures for large near-surface underground structures. In: Proceedings of the 18th international conference on soil mechanics and geotechnical engineering, Paris

Escoffier S (2008) Conteneur ESB. LCPC ınternal report no: 2007-1-13-1/1-a

Ha D, Abdoun TH, O'Rourke MJ et al (2010) Earthquake faulting effects on buried pipelines-case history and centrifuge study. J Earthq Eng 14(5):646–669

Hardin BO, Drnevich VP (1972) Shear modulus and damping in soils: design equation and curves. J Soil Mech Found Eng Div ASCE 98(7):667–692

Hashash Y, Hook JJ, Schmidt B (2001) Seismic design and analysis of underground structures. Tunn Undergr Space Technol 16(4):247–293

Huo H, Bobet A, Fernandez G et al (2006) Analytical solution for deep rectangular underground structures subjected to far field shear stresses. Tunn Undergr Space Technol 21(6):613–625

Iglesia GR, Einstein HH, Whitman RV (2011) Validation of centrifuge model scaling for soil systems via trapdoor tests. J Geotech Geoenv Eng 137(11):1075–1089

Iida H, Hiroto T, Yoshida N, Iwafuji M (1996) Damage to Daikai subway station. Soils Found 36:283–300

Ishibashi I, Zhang X (1993) Unified dynamic shear moduli and damping ratios of sand and clay. Soils Found 33(1):182–191

Lanzano G, Bilotta E, Russo G, Silvestri F, Madabhushi SPG (2012) Centrifuge modeling of seismic loading on tunnels in sand. Geotech Test J 35:854–869

Lee SH, Choo YW, Kim DS (2013) Performance of an equivalent shear beam (ESB) model container for dynamic geotechnical centrifuge tests. Soil dyn Earthq Eng 44:102–114

Li Z, Escoffier S, Kotronis P (2013) Using centrifuge tests data to identify the dynamic soil properties: application to Fontainebleau sand. Soil dyn Earthq. Eng. 52:77–87

Ling HI, Mohri Y, Kawabati T, Liu H, Burke C, Sun L (2003) Centrifugal modeling of seismic behavior of large-diameter pipe in liquefiable soil. J Geotech Geoenviron Eng ASCE 129:1092–1101

Madabhushi SPG (1994) Dynamic response of the equivalent shear beam (ESB) container. İn: Technical report TR270. Department of Engineering, University of Cambridge, Cambridge

O'Rourke M, Gadicherla V, Abdoun T (2003) Centrifuge modeling of buried pipelines. In: Advancing mitigation technologies and disaster response for lifeline systems, proceedings of the 6th U.S. conference and workshop on lifeline earthquake engineering, August 10–13, 2003, Long Beach, pp.757–768

Ozkan MY, Ulgen D, Saglam S, Vrettos C, Chazelas JL (2013) Centrifuge modeling of dynamic behavior of box shaped underground structures in sand. Series Project Web: http://www.series.upatras.gr/sites/default/files/SERIES_Dresbus_Final%20Report.pdf. Accessed July 2013

Pelli E, Yiouta-Mitra P, Sofianos AI (2006) Seismic Behaviour of Square Lined Underground Structures. In: Proceedings of world tunnel congress, Seoul

Penzien J (2000) Seismically induced racking of tunnel linings. J Earthq Eng Struct Dyn 29(5):683–691

Pitilakis K, Tsinidis G, Anastisiadis A, Pitilakis D, Heron C, Madabushi SPG, Stringer M, Paolucci R (2013) Investigation of several aspects affecting the seismic behaviour of shallow rectangular underground structures in soft soils. Series Project Web: http://www.series.upatras.gr/sites/default/files/file/SERIES_TUNNELSEIS_Final_Report.pdf

Power MS, Rosidi D, Kaneshiro JY (1998) Seismic vulnerability of tunnels and underground structures revisited. In: Ozdemir L (ed) Proceedings of the North American tunneling conference, Newport Beach, pp 243-250

Schofield AN (1980) Cambridge geotechnical centrifuge operations. Geotechnique 30(3):227–268

Silver ML, Seed HB (1971) Volume changes in sands due to cyclic loading. J Soil Mech Found Div ASCE 97(9):1171–1182

Sitar N (1995) Geotechnical reconnaissance of the effects of the January 17, 1995, HyogokenNanbu Earthquake, Japan. Earthquake Engineering Research Center, University of California, report no. 95-01

Taylor RN (1995) Geotechnical centrifuge technology. Blackie Academic & Professional, London

Teymur B, Madabhushi SPG (2003) Experimental study of boundary effects in dynamic centrifuge modelling. Geotechnique 53(7):655–663

Tokimatsu K, Seed HB (1987) Evaluation of settlements in sands due to earthquake shaking. J Geotech Eng ASCE 113(8):861–878

Wang JN (1993) Seismic design of tunnels: a state of the art approach. Monograph 7, Parsons, Brinckerhoff, Quade & Diuglas Inc., New York

Wang WL, Wang TT, Su JJ, Lin CH, Seng CR, Huang TH (2001) Assessment of damage in mountain tunnels due to the Taiwan ChiChi Earthquake. Tunn Undergr Space Technol 16(3):133–150

Zeghal M, Elgamal AW (1994) Analysis of site liquefaction using earthquake records. J Geotech Eng ASCE 120(6):996–1017

Zeng X, Schofield AN (1996) Design and performance of an equivalent-shear-beam container for earthquake centrifuge modelling. Geotechnique 46(1):83–102